Surfactant-assisted Hydrothermal Synthesis of Single Phase Pyrite FeS_2 Nanocrystals

Cyrus Wadia[1,2,†], Yue Wu[1,†], Sheraz Gul[3], Steven K. Volkman[4], Jinghua Guo[3], A. Paul Alivisatos[1,5,6,*]

[1]*Department of Chemistry, University of California, Berkeley, CA 94720 USA*

[2] *Energy & Resources Group, University of California, Berkeley, CA 94720 USA*

[3]*Advanced Light Source, Lawrence Berkeley National Laboratory, Berkeley, CA 94720*

[4]*Department of Electrical Engineering and Computer Sciences, University of California, Berkeley, CA 94720 USA*

[5]*Department of Materials Science and Engineering, University of California, Berkeley, CA 94720 USA*

[6]*Materials Science Division, Lawrence Berkeley National Laboratory, Berkeley, CA 94720 USA*

[†] *These authors contribute equally to this work*

Received Date,

Iron pyrite (FeS_2) has long been a material of interest for photovoltaic devices.[1] With an indirect energy transition at 0.95eV, a direct transition at 1.03eV,[1b] and an integrated absorption coefficient of 3.3×10^5 cm^{-1} for the energy spectrum of wavelength values (λ) between 300 nm and 750 nm, it is ideally suited for photovoltaic applications. This coupled with low procurement costs and vast abundance gives pyrite the potential to be a disruptive photovoltaic material when compared to many other candidate. [2] Numerous iron sulfides exist in nature, each with unique magnetic and electrical properties that are strongly related to the stoichiometric ratio between Fe and S as well as crystalline structure. Pyrite has previously been prepared using several high temperature approaches including: MOCVD, sulfurization of iron films, sulfurization of iron oxide films, reactive sputtering and spray pyrolysis,[3,1b] Yet at elevated temperatures, segregation of iron and sulfur species is unavoidable, which could change the stoichiometry and material phase of the deposited film. In fact, the best demonstrated pyrite photovoltaic device by these techniques shows a modest 2.8% power conversion efficiency.[1a] This low performance was partially explained by a high density of surface defects, but the unusually low open circuit voltage of 200 mV suggests that phase purity may also play a role.[1,3] Orthorhombic marcasite FeS_2 and hexagonal troilite FeS are both common iron sulfur phases but because they have much smaller band gaps (0.34 eV for marcasite and 0.04 eV for troilite), even trace amounts would explain the low open circuit voltage observed in this previous work.

Semiconductor nanocrystals have been used as building blocks to assemble a range of electronic and photonic structures, including light emitting diodes, lasers, and photovoltaics.[4] Critical to the functionality of these types of devices are the purity, crystallinity, stoichiometry, and size of the nanocrystal building blocks. While some low temperature solution phase colloidal nanocrystal synthesis approaches to pyrite have been explored,[5] these efforts are early and unlike their thin film predecessors, there are no reports on photovoltaics made from these synthetic materials.

Single source molecular precursors with precisely defined composition can provide a high degree of control of nanocrystal synthesis, as demonstrated with the growth of CdS, ZnS, CdSe, ZnSe, Sb_2Te_3, In_2S_3 nanocrystals[6] as well

(1) (a) Ellmer, K.; Tributsch H. In *Iron Disulfide(Pyrite) as Photovoltaic Material: Problems and Opportunities*, Proceedings of the 12th Workshop on Quantum Solar Energy Conversion, Wolkenstein Suditrol, Italy, May 11 - 18, 2000; Wolkenstein Suditrol, Italy, 2000. (b) Ennaoui, A.; Fiechter, S.; Pettenkofer, C.; Alonsovante, N.; Buker, K.; Bronold, M.; Hopfner, C.; Tributsch, H., Iron Disulfide for Solar-Energy Conversion. *Solar Energy Materials and Solar Cells* **1993,** 29, (4), 289-370. (c)Altermatt, P.; Kiesewetter, T.; Ellmer, K.; Tributsch, H., Specifying targets of future research in photovoltaic devices containing pyrite (FeS2) by numerical modelling. *Solar Energy Materials and Solar Cells* **2002,** 71, (2), 181-195. (d) Chatzitheodorou, G.; Fiechter, S.; Konenkamp, R.; Kunst, M.; Jaegermann, W.; Tributsch, H., Thin Photoactive Fes2 (Pyrite) Films. *Materials Research Bulletin* **1986,** 21, (12), 1481-1487 (e) Ennaoui, A.; Tributsch, H., Iron Sulfide Solar-Cells. *Solar Cells* **1984,** 13, (2), 197-200. (f) Ennaoui, A.; Tributsch, H., Energetic Characterization of the Photoactive Fes2 (Pyrite) Interface. *Solar Energy Materials* **1986,** 14, (6), 461-474. (g) Nesbitt, H.W.; Bancroft, G.M.; Pratt, A.R.; Scaini, M.J., Sulfur and iron surface states on fractured pyrite surfaces. *American Mineralogist* **1998**, 83, 1067-1076.

(2) Wadia, C.; Alivisatos, A. P.; Kammen, D., Materials Availability Expands the Opportunity for Large-Scale Photovoltaics Deployment. *Environ. Sci. Technol.* **2009,** 43, (6), 2072-2077.

(3) Luther, G., Pyrite Synthesis Via Polysulfide Compounds. *Geochimica Et Cosmochimica Acta* **1991,** 55, (10), 2839-2849

(4) (a) Coe, S.; Woo, W. K.; Bawendi, M.; Bulovic, V., Electroluminescence from single monolayers of nanocrystals in molecular organic devices. *Nature* **2002,** 420, (6917), 800-803. (b) Klimov, V. I.; Mikhailovsky, A. A.; Xu, S.; Malko, A.; Hollingsworth, J. A.; Leatherdale, C. A.; Eisler, H. J.; Bawendi, M. G., Optical gain and stimulated emission in nanocrystal quantum dots. *Science* **2000,** 290, (5490), 314-317. (c) Sun, S. H.; Murray, C. B., Synthesis of monodisperse cobalt nanocrystals and their assembly into magnetic superlattices (invited). *Journal of Applied Physics* **1999,** 85, (8), 4325-4330. (d) Huynh, W. U.; Dittmer, J. J.; Alivisatos, A. P., Hybrid nanorod-polymer solar cells. *Science* **2002,** 295, (5564), 2425-2427.

(5) (a)Chen, X. H.; Fan, R., Low-temperature hydrothermal synthesis of transition metal dichalcogenides. *Chemistry of Materials* **2001,** 13, (3), 802-805. (b) Chen, X. Y.; Wang, Z. H.; Wang, X.; Wan, J. X.; Liu, J. W.; Qian, Y. T., Single-source approach to cubic FeS2 crystallites and their optical and electrochemical properties. *Inorganic Chemistry* **2005,** 44, (4), 951-954. (c) Duan, H.; Zheng, Y. F.; Dong, Y. Z.; Zhang, X. G.; Sun, Y. F., Pyrite (FeS2) films prepared via sol-gel hydrothermal method combined with electrophoretic deposition (EPD). *Materials Research Bulletin* **2004,** 39, (12), 1861-1868. (d) Kar, S.; Chaudhuri, S., Solvothermal synthesis of nanocrystalline FeS2 with different morphologies. *Chemical Physics Letters* **2004,** 398, (1-3), 22-26. (e) Kar, S.; Mandal, S. K.; Das, D.; Chaudhuri, S., Wet chemical synthesis of iron pyrite and characterization by Mossbauer spectroscopy. *Materials Letters* **2004,** 58, (22-23), 2886-2889. (f) Xuefeng, Q., Xie, Y., Yitai, Q., Solventothermal synthesis and morphological control of nanocrystalline FeS2 *Materials Letters* **2001,** 48, 109-111.

(6) (a) O'Brien, P.; Walsh, J. R.; Watson, I. M.; Hart, L.; Silva, S., Properties of cadmium sulphide films grown by single-source metalorganic chemical vapour deposition with dithiocarbamate precursors. *Journal of Crystal Growth* **1996,** 167, (1-2), 133-142. (b) Cumberland, S. L.; Hanif, K. M.;

as the growth of CdS and ZnS nanowires.[7] Herein, we report the use of single-source molecular precursors for the growth of single phase FeS_2 pyrite nanocrystals through a hydrothermal reaction. Surfactant selection and control of solution pH have been found to play key roles in the preparation of single phase iron pyrite.

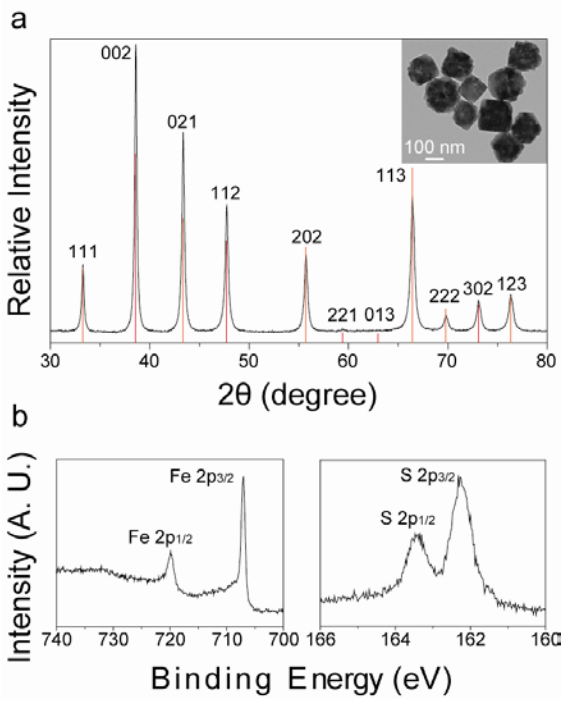

Figure 1. (a) XRD pattern and TEM image and (b) XPS spectra of pure pyrite FeS_2 yielded from hydrothermal synthesis.

Our synthetic approach starts with the formation of the single source molecular precursor iron (III) diethyl dithiophosphate ($[(C_2H_5O)_2P(S)S]_3Fe$) in aqueous solution through the reaction between iron (III) chloride ($FeCl_3$) and diethyl dithiophosphate ammonium salt ($(C_2H_5O)_2P(S)SNH_4$) (formation of this product was confirmed through mass spectrometry studies and is detailed in the supplemental information). Then, the single source precursor with the addition of hexadecyltrimethylammonium bromide (CTAB) acting as a surfactant undergoes thermal decomposition by a hydrothermal reaction in a 125ml teflon lined stainless steel acid digestion bomb at 200 ^oC. We also demonstrate an alternative approach where the molecular precursor may be formed in-situ and is detailed in the supplemental informaion.

XRD studies (Fig. 1a) show the materials prepared in this way are cubic pyrite FeS_2 (JCPDS 03-065-1211, Fig. 1a red lines) without any noticeable impurity peaks from orthorhombic marcasite FeS_2 or hexagonal troilite FeS. Transmission electron microscopy (TEM) studies (inset, Fig. 1a) show large quasi-cubic nanocrystal agglomerations with an average size over 100 nm. The pyrite nanocrystals were further investigated through X-ray photoelectron spectroscopy (XPS) (Fig. 1b). Iron peaks in the XPS spectrum are associated with FeS_2. The Fe $2p_{3/2}$ binding energy of 707 eV (Fig. 1b, left panel) is characteristic of pyrite (with no observable impurities from troilite). The S $2p_{3/2}$ and S $2p_{1/2}$ peaks at 162.28 eV and 163.47 eV respectively (Fig. 1b, right panel), are also consistent with the sulfur binding energy in bulk pyrite.[1g]

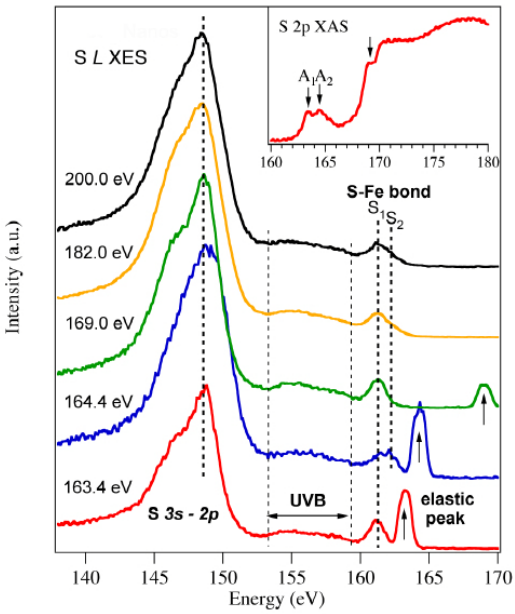

Figure 2. X-ray absorption spectrum of nanostructured FeS_2 (inset) and resonant excited X-ray emission spectra of S L-edges with the excitation energy indicated by the notations and arrows in the XAS spectrum.

To elucidate their electronic structure, the FeS_2 nanocrystals have been studied by X-ray absorption spectroscopy (XAS) and X-ray emission spectroscopy (XES). XAS probes the local unoccupied electronic structure (conduction band); XES probes the occupied electronic structure (valence band); and the addition of resonant inelastic X-ray scattering (Raman spectroscopy with X-rays) can provide significant insight into the energy levels that reflect the chemical and physical properties of semiconductors.[8] The experiment was performed on BL7 at the Advanced Light Source, Lawrence Berkeley National

Javier, A.; Khitrov, G. A.; Strouse, G. F.; Woessner, S. M.; Yun, C. S., Inorganic clusters as single-source precursors for preparation of CdSe, ZnSe, and CdSe/ZnS nanomaterials. *Chemistry of Materials* **2002,** 14, (4), 1576-1584. (c) Crouch, D. J.; O'Brien, P.; Malik, M. A.; Skabara, P. J.; Wright, S. P., A one-step synthesis of cadmium selenide quantum dots from a novel single source precursor. *Chemical Communications* **2003**, (12), 1454-1455. (d) Revaprasadu, N.; Malik, M. A.; O'Brien, P.; Zulu, M. M.; Wakefield, G., Single-source molecular precursors for the deposition of zinc selenide quantum dots. *Journal of Materials Chemistry* **1998,** 8, (8), 1885-1888. (e) Garje, S. S.; Eisler, D. J.; Ritch, J. S.; Afzaal, M.; O'Brien, P.; Chivers, T., A new route to antimony telluride nanoplates from a single-source precursor. *Journal of the American Chemical Society* **2006,** 128, (10), 3120-3121. (f) Afzaal, M.; Crouch, D.; Malik, M. A.; Motevalli, M.; O'Brien, P.; Park, J. H., Deposition of CdSe thin films using a novel single-source precursor; [MeCd{((SePPr2)-Pr-i)(2)N}](2). *Journal of Materials Chemistry* **2003,** 13, (4), 639-640.

(7) Barrelet, C. J.; Wu, Y.; Bell, D. C.; Lieber, C. M., Synthesis of CdS and ZnS nanowires using single-source molecular precursors. *Journal of the American Chemical Society* **2003,** 125, (38), 11498-11499.

(8) Guo, J., X-ray Absorption and Emission Spectroscopy in Nanoscience and Lifesciences. In *Nanosystem characterization Tools in the Life Sciences*, Kumar, C., Ed. Wiley-VCH Verlag GmbH & Co. KgaA: Weinheim, 2006; pp 259-291.

Laboratory. The resolution was set to 0.1 eV for XAS and 0.2 eV for XES.

The X-ray absorption and emission spectra of nanostructured iron pyrite were recorded at the S L-edge and Fe L-edge. The S 2p XAS spectrum (Fig. 2, inset) reflects the density of states of the conduction band. The spin orbit splitting of about 1.2 eV is also reflected in the XAS spectrum, indicated as A1 and A2. The non-resonant excited S L-edge XES spectrum (Fig. 2) shows the density of states of the valence band. The intensive band around 145-150 eV arises predominantly from levels with 3s character, while the upper valence band (UVB) being mostly of 3p character shows a much weaker intensity due to the dipole selection rule of the XES process. The small band close to the Fermi level at around 161 eV is attributed to S 3d states that are hybridized with Fe 3d states. Its asymmetric shape indicates the two components due to the valence states projected on L shell vacancies with spin orbital splitting of 1.2 eV for $2p_{3/2}$ and $2p_{1/2}$. When resonantly exciting A1 and A2 in the XAS spectrum, one can see the resonant enhancement for each corresponding component S1 and S2.

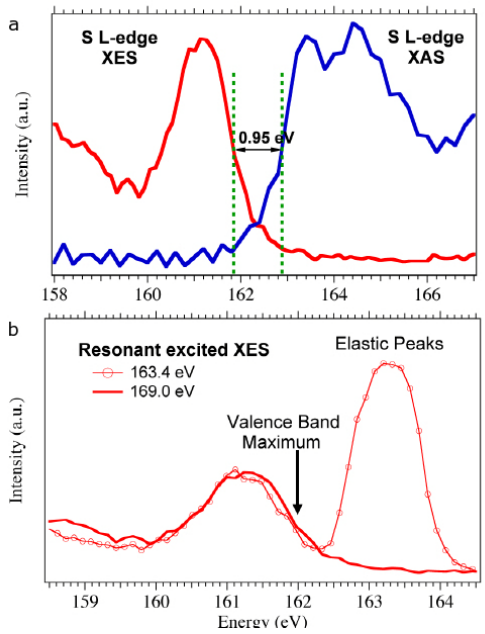

Figure 3. (a) The top of valence band and bottom of conduction band indicating the bandgap of 0.95 eV; (b) the shift of top of valence band from resonantly excited XES spectra suggesting an indirect bandgap in nanostructured FeS_2.

To determine the bandgap from the valence band maximum (VBM) to the conduction band minimum (CBM), we plot the resonantly excited S L-edge XES spectrum (excited at 169 eV) together with S 2p XAS spectrum (Fig. 3a). The bandgap is 0.95 ± 0.1 eV as indicated in the figure. Resonant X-ray emission spectroscopy has also been used to determine the direct or indirect bandgap of semiconductors.[9]

In a simplified picture, one can say that the position of the electron in the CB band structure after the XAS event will select which VB electrons can participate in the XES process. The experimental handle to access band structure information is the excitation energy. Figure 3b shows that emission at the highest energy is not obtained for excitation at threshold, which suggests an indirect bandgap in the nanostructured FeS_2.

In order to gain further insight into the mechanisms and nature of our synthesis, a number of synthetic variations were performed (see supporting information). These variants included: reaction temperature, reaction time, solution pH, and surfactants (primary, secondary or tertiary mixtures). Slightly acidic conditions and the presence of a halogenated cetrimonium were critical in the formation of the pure phase of pyrite. Other parameters, including reaction time and co-surfactant, have been found to have little effect on the purity. Notably, when long chain alkylamines for example oleylamine, are used as a co-surfactant, smaller and more cubic-shaped nanocrystals can be obtained but at the expense of purity in which XRD patterns begin to show marcasite peaks. A detailed reaction mechanism is still under investigation.

In conclusion, we have demonstrated a single-source molecular precursor that can be used for the synthesis of single phase pyrite FeS_2 nanocrystals. Characterization confirms an indirect transition and a bandgap of 0.95 eV. The reaction temperature, pH value, precursor, and surfactant have been found to play important roles in the control of material purity. These single phase pyrite FeS_2 nanocrystals represent a good candidate material for studies of nanoscale photovoltaic solar cells based on non-toxic and earth abundant materials.

Acknowledgement. We thank Timothy Teague, Wanli Ma, Jonathan S. Owen, Michael Geier, Elena Schevchenko, and Dmitri Talapin for helpful discussions. Cyrus Wadia thanks the Environmental Protection Agency for the EPA STAR Fellowship. Yue Wu thanks the Miller Institute for Basic Research in Science for Miller Research Fellowship. This work was supported by the Director, Office of Science, Office of Basic Energy Sciences, Materials Sciences and Engineering Division, of the U.S. Department of Energy under Contract No. DE-AC02-05CH11231.

Supporting Information Available: Detailed procedures about experiments, molecular structure and mass spectrum of the molecular precursor, XPS spectrum of the pyrite FeS_2 nanocrystals and TEM images of nanocrystals containing marcasite impurities synthesized using CTAB and oleylamine mixture. This material is available free of charge via the Internet at http://pubs.acs.org.

(9) Eisebitt, S.; Luning, J.; Rubensson, J. E.; Eberhardt, W., Resonant inelastic soft X-ray scattering as a bandstructure probe: A primer. *Physica Status Solidi B-Basic Research* **1999,** 215, (1), 803-808.

DISCLAIMER